IJBPAS, November, 2021, 10(11): 3785-3798

ISSN: 2277–4998

International Journal of Biology, Pharmacy and Allied Sciences (IJBPAS)

'A Bridge Between Laboratory and Reader'

www.ijbpas.com

DESIGN, COMPUTATIONAL, SYNTHESIS, CHARACTERIZATION AND MOLECULAR DOCKING ASSESMENT OF 1,2,4-TRIAZOLE MOIETIES

INGOLE PARAG G*, PANCHABHAI VIVEK B[1] AND BUTLE SANTOSH R[1]

School of Pharmacy, Swami Ramanand Teerth Marathwada University, Nanded-431606, Maharashtra, India

***Corresponding Author: Dr. Ingole Parag G: E Mail: ingoleparag@gmail.com**

Received 7th Jan. 2021; Revised 9th Feb. 2021; Accepted 5th March 2021; Available online 1st Nov. 2021

https://doi.org/10.31032/IJBPAS/2021/10.11.5687

ABSTRACT

EGFR has been found to be expressed and altered in a variety of malignancies and clearly it plays a significant role in tumor development and progression, including cell proliferation, regulation of apoptotic cell death, angiogenesis and metastatic spread. A series of 4-substituted amino-5-Substituted-4H-1,2,4-triazole-3-thiol derivatives were designed for molecular modelling studies. Molecular docking study was performed to check the receptor and ligand interaction or binding affinity by using the receptor 1M17. Some of designed molecules were found to have binding affinity comparable with the cocrystalized ligand AQ4. Molecules with good binding affinity were synthesized and confirmed for their structure by IR, NMR and Mass.

Keywords: Epidermal growth factor, Receptor tyrosine kinase, Cancer therapy, docking

INTRODUCTION

The epidermal growth factor (EGFR) belonging to the family of Receptor tyrosine kinase (RTKs) also called as phosphotyrosinekinase **[1]**. Receptor tyrosine kinase are single pass transmembrane protein important in intercellular signaling, by translating extracellular signals (ligands or growth factors) into activation of specific cell signaling cascades i.e. they plays an important role in signal transduction pathways that regulate cell division and differentiation **[2]**. The receptor tyrosine kinase family comprises of four members:

EGFR (HER-1/ErbB-1), HER-2 (ErbB-2), HER-3 (ErbB-3) and HER-4 (ErbB-4) **[3]**.

The Tyrosine kinase receptors are known to be activated by binding to different ligands (including EGF, TGFA) after a ligand binds to the extracellular domain of the receptor, the receptor forms functionally active dimers (EGFR-EGFR (homodimer) or EGFR-HER2, EGFR-HER3, EGFR-HER4 (heterodimer) **[4]**. Dimerization induces the activation of the tyrosine kinase domain, which leads to autophosphorylation of the receptor on multiple tyrosine residues. This leads to activation a series of intracellular signaling cascades to affect gene transcription, which in turn results in cancer cell proliferation, reduced apoptosis, invasion and metastasis and also stimulates tumor-induced angiogenesis **[5]**.

EGFR has been found to be expressed and altered in a variety of malignancies and clearly it plays a significant role in tumor development and progression, including cell proliferation, regulation of apoptotic cell death, angiogenesis and metastatic spread **[6]**. EGFR tyrosine kinase-mediate cell growth signaling pathways plays an important role in the formation and development of many types of solid tumors, including head and neck, lung, breast, bladder, prostate and kidney cancers **[7]**. Therefore, EGFR tyrosine kinase represents an attractive target for the development of novel anticancer agents. EGFR and HER-2 are the hottest targets in current cancer research and their over expression or abnormal activation often cause cell malignant transformation. Gefitinib and Erlotinib are the representative drugs for this kind of inhibitors and have been approved by US FDA for the treatment of patient with non-small-cell-lung cancer (NSCLC) **[8]**.

1,2,4-triazole derivatives have attracted continuing interest over the years because of their varied biological activities, such as anti-inflammatory, antimicrobial, anti-proliferative, antiviral, anticonvulsant, anti-fungal and antibacterial and anticancer agents **[9]**. Thus, a series of newly designed 1,2,4-triazole derivatives were chosen for docking studies. Molecules with good binding affinity were synthesized and structure confirmation done by IR, NMR and Mass spectral studies.

EXPERIMENTAL

Materials and Methods

All docking calculations were carried out on PC having configuration intel core i3-4130 3.40 GHz processor, Operating System - Linux and 4 GB RAM. Average time required for docking was 0.6 min/ molecule in the XP mode. The Maestro (version 10.2, Schrödinger, LLC, New York, NY, 2015) software was used to dock potential inhibitors (Ligand) in the binding pocket of the enzyme structure.

Glide is most commonly used and validated software designed to assist in high-throughput screening of potential ligands based on binding mode and affinity for a given receptor molecule.

All starting and raw chemicals of brand S. D. Fine Chemicals (Mumbai, India) were purchased from local supplier. All chemicals were of LR Grade. Solvents used were of GR grade. Progress of the reaction and purity of the compounds was confirmed by Merck precoated aluminium TLC plates by using appropriate mobile phase and spots were rendered visible by exposing to UV light and iodine fumes. The products of all the reactions were purified initially by different workup processes and recrystallization using suitable solvents. The absence of any impurity of starting material or possible by-product was ensuring by performing single TLC spot of product. Melting points were determined in open capillaries using melting point apparatus (VEEGO VMP-D) and reported as uncorrected. IR spectra (KBr) were recorded on FTIR-8400s spectrophotometer (Shimadzu, Japan). ^{1}HNMR spectra were recorded by Varian-NMR-Mercury 300 using $CDCl_3$ as a solvent and their chemical shifts are recorded in δ parts per million (ppm) units with respect to tetramethylsilane (TMS) as an internal standard at Central Instrumentation Lab, Savitribai Phule Pune University, Pune. Compounds were further characterized by liquid chromatography–electrospray ionization mass spectrometry (LC–ESI/MS) with accurate mass measurements upto four decimals.

1. Receptor Selection:

Docking studies were carried out using epidermal growth factor receptor 1M17 with a selective inhibitor, aq-4 ([6,7-bis (2-methoxy-ethoxy) quinazoline-4-yl]-(3-ethynylbenzyl) amine). It was solved by X-ray diffraction techniques. We retrieved it from the Brookhaven protein database **[10]**. All potential ligands were drawn using build panel in maestro graphical user interface. The number of ligands was designed maintaining diversity of substituents on the basic template **(Figure 1)** for docking are listed in **Table 1** given below.

2. Ligand Preparation:

Ligand preparation was carried out using LigPrep panel in the software. The use of LigPrep produces a single low-energy 3D structure with correct chiralities for each successfully processed input structure. All the structures in .mae format were imported in the project file and subjected to ligand preparation using OPLS 2005 force field.

Possible ionization states for each structure at the pH 7.0 ± 2.0 were generated using the ionizer option and only one low energy ring conformer per ligand was allowed to

generate. Low energy stereoisomer 01 per ligand was allowed to generate.

3. Protein and Ligand Complex Preparation:

The quality of the results obtained from Glide depends critically on the quality of the starting structures. These starting structures must include all hydrogens, have correct charge states near the binding site, and be reasonably free of major steric clashes. A typical PDB protein complex structure, as downloaded from the Research Collaboratory for Structural Bioinformatics (RCSB) web site (http://www.rcsb.org), has no hydrogens and may have residues in unusual charge states. Therefore, comprehensive protein preparation to ensure chemical correctness and optimization of protein structure was done in order to achieve best results. All water molecules were deleted.

It is necessary that ligand, cofactors and nonstandard residues have appropriate bond orders and formal charges so bond order or formal charges were adjusted using toolbars in the maestro graphical user interface.

Protein Preparation and refinement was carried out keeping Neutralization zone around the ligand 'On' and RMSD of 0.30 Å. During the preparation stage, hydrogen treatment is applied to the ligand and the protein. Residues within 10–20 Å of the ligand are neutralized. A series of restrained partial minimizations of the cocrystallized complex to optimize the positions of the newly added hydrogens and relieve any strain due to unphysical short distances in the X-ray structure was carried out under refinement portion. The optimized 1M17 enzyme structure and structure of cocrystalized ligand AQ4 is shown in **Figure 2 A and Figure 2 B**, respectively.

4. Receptor Grid Generation:

Grid files represent physical properties of a volume of the receptor, specifically the active site that will be searched when attempting to dock a ligand. This grid file calculated is used to dock ligands in the next step.

The purple enclosing box represents the volume of the protein for which grids will be calculated as shown in **Figure 3**. Center option selected is Centroid of Workspace ligand. Size option selected is the default, which is Dock ligand similar in size to the Workspace ligand. No constraints were selected for grid preparation

5. Ligand Docking:

Docking was carried out using XP (Extra precision) mode. Flexible docking with flips of 5- and 6-member rings was allowed. Docking and scoring of potential two sets of ligands was carried out without calculating or using similarity scores. Additional filters were also used. Settings were done so that ligands with more than

120 atoms and 20 rotatable bonds will not be docked and one pose for each ligand was collected and written to the pose viewer file. A Van der Waals radius scaling for ligand atoms is set to the default values: Scale by 0.80 atoms with partial atomic charge less than 0.15.

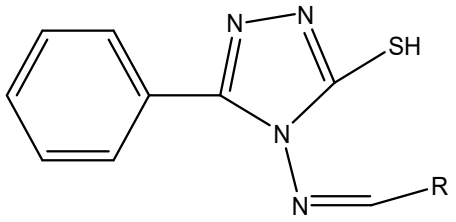

Figure 1: PGI series of derivatives containing 54 compounds

Table 1: PGI series containing 54 compounds

S. No.	Comp. code	R	SN	Comp. code	R
1	PGI 1	Benzyl	28	PGI 28	3 -F, 4 -Br Benzyl
2	PGI 2	4-Cl Benzyl	29	PGI 29	2 -F, 5 -Br Benzyl
3	PGI 3	3-NO_2 Benzyl	30	PGI 30	4-bromofuran-2-yl
4	PGI 4	2,3,4 tri OH Benzyl	31	PGI 31	5-bromofuran-2-yl
5	PGI 5	2, 4 di-OH Benzyl	32	PGI 32	5-nitrofuran-2-yl
6	PGI 6	3-OH Benzyl	33	PGI 33	3 -Br, 4 – OCH_3Benzyl
7	PGI 7	2-F Benzyl	34	PGI 34	2 – OCH_3, 4 -Br Benzyl
8	PGI 8	3,4-di OH Benzyl	35	PGI 35	2 – OCH_3, 5 -Br Benzyl
9	PGI 9	3,4 di F Benzyl	36	PGI 36	2 -OH, 3 – Br, 5 -NO_2 Benzyl
10	PGI 10	2 -CH_3 Benzyl	37	PGI 37	2 -OH, 3 – NO_2, 5 -Br Benzyl
11	PGI 11	3 -CH_3 Benzyl	38	PGI 38	2 -OH, 3 – CF_3 Benzyl
12	PGI 12	2,4 di -CH_3 Benzyl	39	PGI 39	2-bromopyridin-4-yl
13	PGI 13	2,4,5 tri OH Benzyl	40	PGI 40	5-bromopyridin-2-yl
14	PGI14	2, 4 -di CF_3 Benzyl	41	PGI 41	5-bromopyridin-3-yl
15	PGI 15	2, 5 -di CF_3 Benzyl	42	PGI 42	6-bromopyridin-2-yl
16	PGI 16	3, 5 -di CF_3 Benzyl	43	PGI 43	2,3,4 -tri OCH_3 Benzyl
17	PGI 17	2 -Br Benzyl	44	PGI 44	3,4,6 -tri OCH_3 Benzyl
18	PGI 18	3 -Br Benzyl	45	PGI 45	2,4,6 -tri OCH_3 Benzyl
19	PGI 19	4 -Br Benzyl	46	PGI 46	3,4,5 -tri OCH_3 Benzyl
20	PGI 20	2 -Cl, 4 – Br Benzyl	47	PGI 47	4 -SCF_3 Benzyl
21	PGI 21	2 -Br, 3 -F, 6- F Benzyl	48	PGI 48	2 – NO_2 Benzyl
22	PGI 22	2 -F, 3 -Br, 6- F Benzyl	49	PGI 49	4 – NO_2 Benzyl
23	PGI 23	3 -F, 4 -Br, 6- F Benzyl	50	PGI 50	2- Cl, 3 -F Benzyl
24	PGI 24	2 -F, 3 -F, 6- Br Benzyl	51	PGI 51	2- Cl, 4 -F Benzyl
25	PGI 25	3 -F, 6- Br Benzyl	52	PGI 52	2- Cl, 6 -F Benzyl
26	PGI 26	3 -Br, 4 -F Benzyl	53	PGI 53	2 -F, 3- Cl Benzyl
27	PGI 27	2 -F, 4 -Br Benzyl	54	PGI 54	3- Cl, 4-F Benzyl

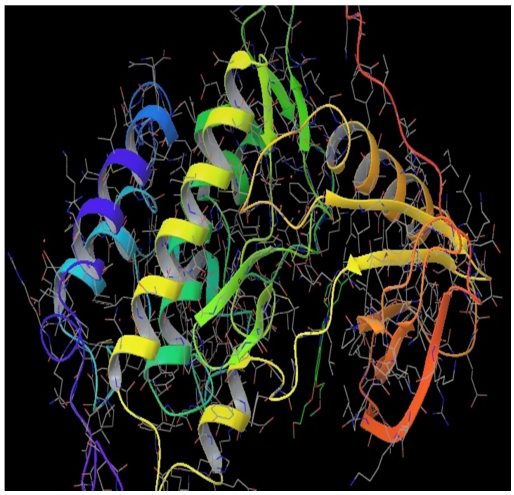

Figure 2A: 1M17 enzyme structure

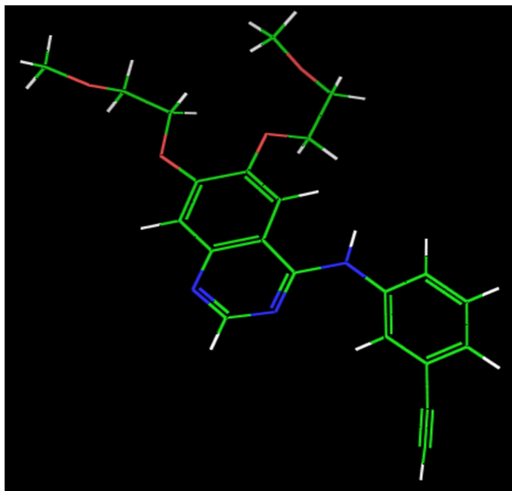

Figure 2B: Cocrystalized ligand AQ4

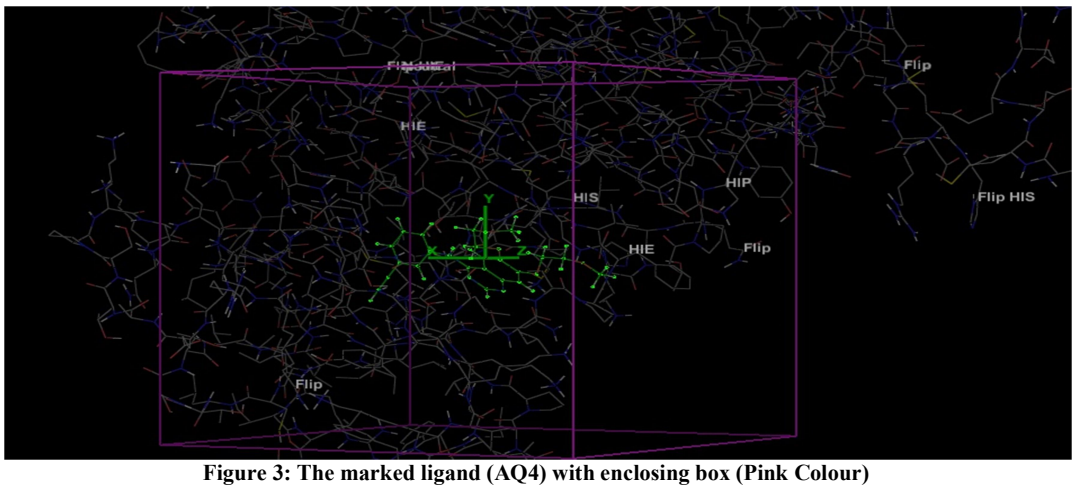

Figure 3: The marked ligand (AQ4) with enclosing box (Pink Colour)

RESULTS AND DISCUSSION

The combination of position and orientation of a ligand relative to the receptor, along with its conformation in flexible docking, is referred to as a *ligand pose*. The ligand poses that Glide generates pass through a series of hierarchical filters that evaluate the ligand's interaction with the receptor. The initial filters test the spatial fit of the ligand to the defined active site, and examine the complementarity of ligand-receptor interactions using a grid-based method Poses that pass these initial screens enter the final stage of the algorithm, which involves evaluation and minimization of a grid approximation to the OPLS-AA nonbonded ligand-receptor interaction energy. Final scoring is then carried out on the energy-minimized poses. Glide results are examined with an emphasis on visual rather than numerical appraisal. The glide results are viewed through glide pose viewer panel. For each pose, the table gives the Glide Score (G-Score) and Glide Energy, and various contact counts associated with the pose-

receptor combination. Results for top 15 molecules from PGI series is shown in the **Table 2**.

For viewing the results of docking, compounds from the two series has been selected according to the best scored conformation predicted by the Glide scoring function. The interaction of these ligands has been shown in **Figures 4 to Figure 6**.

Table 2: Extra precision docking results for compounds belonging to PGI Series

SN	Molecule ID	Docking score/ Glide Score	Glide energy
1	PGI 48	-6.932	-47.277
2	PGI 14	-6.888	-37.746
3	PGI 15	-6.773	-41.066
4	PGI 8	-6.385	-41.946
5	PGI 16	-6.212	-40.788
6	PGI 38	-6.177	-39.702
7	PGI 25	-6.023	-38.301
8	PGI 53	-5.94	-36.297
9	PGI 51	-5.913	-40.379
10	PGI 43	-5.84	-40.804
11	PGI 5	-5.813	-42.349
12	PGI 54	-5.749	-38.034
13	PGI 30	-5.704	-41.646
14	PGI 37	-5.69	-43.393
15	PGI 3	-5.686	-37.747

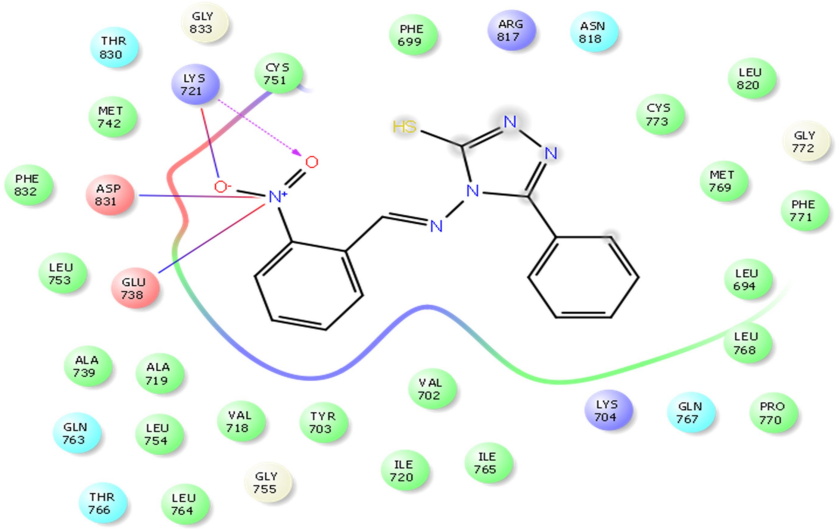

Figure 4: Binding of PGI 48 into the active site of 1M17 enzyme.

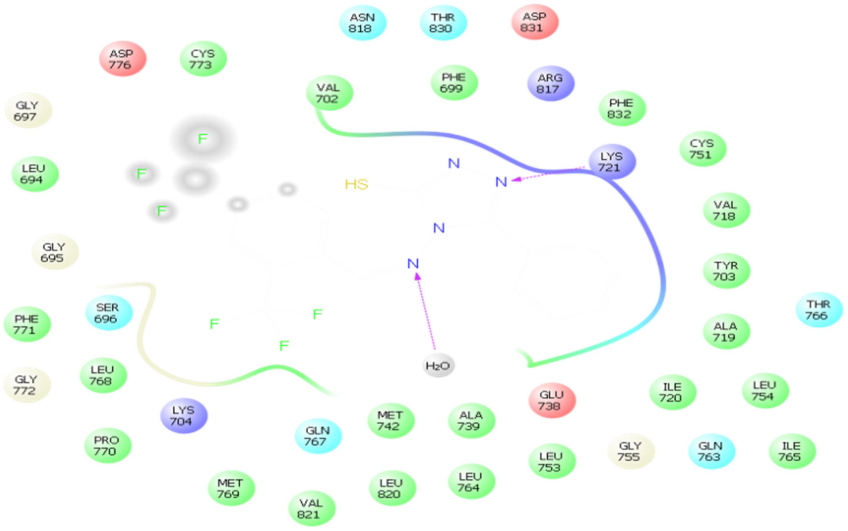

Figure 5: Binding of PGI 14 into the active site of 1M17 enzyme

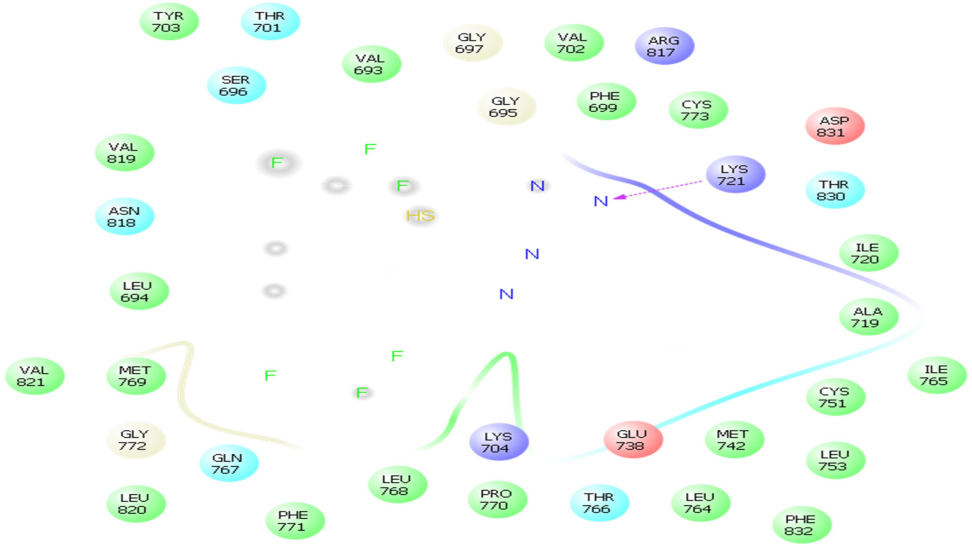

Figure 6: Binding of PGI 15 into the active site of 1M17 enzyme

SYNTHESIS OF 4-SUBSTITUTED AMINO-5-PHENYL-4H-1,2,4-TRIAZOLE-3-THIOL DERIVATIVES [11, 12]

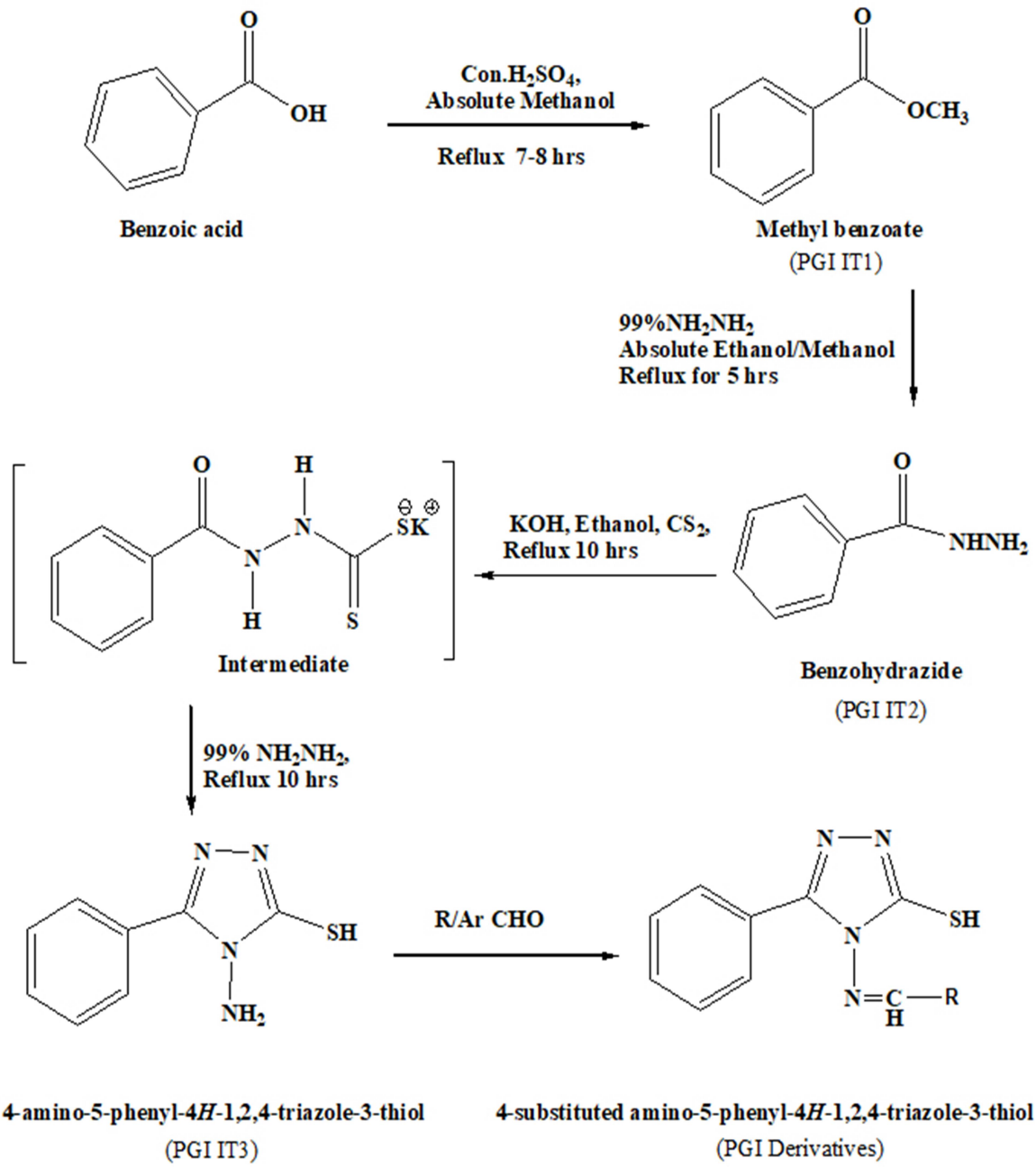

Figure 7: Scheme of Synthesis for PGI Series compounds

Step 1: -Procedure of Synthesis of Ester from Acid (PGIIT 1): -

Take 0.1 mole of Benzoic acid to dry RBF. Add 30 ml of dried methanol. Dissolves the acid in solvent. Add 0.1 mol of conc. H_2SO_4 drop wise with mechanical stirrer. Reflux the reaction mixture for 7-8 hrs at 50-60^{0}c. After reflux, allow to cool.

Meanwhile prepare saturated solution of 10% Sodium Bicarbonate ($NaHCO_3$). When reaction mixture is cooled than reflux temperature, pour mixture to large beaker. Add solution of $NaHCO_3$ to make pH neutral. Mixture will give effervesces of CO_2 but latter it will be reduced and product of ester will be obtained.

Yield: 92.48%. Bp: 198-201°C. IR (KBr) cm^{-1}: 2942, 1715, 1635, 1180. ^1H NMR (DMSO-d6, 400 MHz) δ: 3.95 (s, 3H, CH_3), 7.38-7.77 (s, 2H, NH_2). HRMS (EI) m/z calcd for $C_8H_8O_2$ 136.15, found 136.5.

Step 2: Procedure of Synthesis of Hydrazide from Ester (PGIIT 2): -

To a solution of ester (1 mmol, 1 equiv.), 99% hydrazine hydrate (3 mmol, 3.0 equiv.) was added drop-wise. The reaction mixture was refluxed for 5 hrs at 50^0C; after completion of the reaction, a solid product was formed, and the excess solvent was removed under reduced pressure.

Yield: 79.48%. mp: 231-233°C. IR (KBr) cm^{-1}: 3384, 3410, 2568, 1592. ^1H NMR (DMSO-d6, 400 MHz) δ: 1.78 (s, 2H, NH_2), 2.34 (s, 1H, SH), 7.44-7.62 (m, 1H, Ar). HRMS (EI) m/z calcd for $C_7H_8N_2O$ 192.24, found 192.24.

STEP 3: Procedure of Synthesis of Triazole from Hydrazide (PGIIT 3): -

To the Solution of Potassium hydroxide (1.5 mmol, 1.5 equiv.) and absolute ethanol (25mL); Substituted hydrazine (1 mmol, 1 equiv.), and carbon disulphide (1.5 mmol, 1.5 equiv.) were added drop-wise, mixture was refluxed for 10hrs. After completion of the reaction, the solvent was evaporated under reduced pressure, and the intermediate residue was obtained. To the crude residue 99% Hydrazine Hydrate (25 ml) was added and refluxed for 10 hrs. The reaction mixture was acidified with 10% HCl solution which give precipitate. The precipitate was filtered, washed with water, and dried **[3]**.

Yield: 85.96%. mp: 223-235°C. IR (KBr) cm^{-1}: 3355, 3376, 2568, 1592, 1343. ^1H NMR (DMSO-d6, 400 MHz) δ: 1.78 (s, 2H, NH_2), 2.34 (s, 1H, SH), 7.44-7.62 (m, 1H, Ar). HRMS (EI) m/z calcd for $C_8H_8N_4S$ 192.24, found 192.24.

Step 4: -Procedure of Synthesis of 4-substituted amino-5-phenyl-4H-1,2,4-triazole-3-thiol from Triazole (PGI derivative): **-:**

A mixture of 4-amino-5-phenyl-4H-1,2,4-triazole-3-thiol (0.96 g, 0.005 mol) and substituted aldehydes (0.005 mol) in ethanol (25 mL) was refluxed for 4 hrs then, after cooling, was diluted with H_2O (20 mL). The crude product thus obtained will be collected by filtration.

PGI 3:- 4-[(*E*)-(3-nitrophenyl)diazenyl]-5-phenyl-4*H*-1,2,4-triazole-3-thiol

Yield: 80.50%. mp: 220-223°C. IR (KBr) cm^{-1}: 3072, 3376, 2594, 1676, 1348. ^1H NMR (DMSO-d6, 400 MHz) δ: 2.75 (s, 2H, SH), 7.36-8.11 (m, 1H, Ar), 7.93 (s,

1H, CH). HRMS (EI) m/z calcd for $C_{15}H_{11}N_5O_2S$ 325.25, found 325.25.

PGI 5:- 4-[(*E*)-(3-phenyl-5-sulfanyl-4*H*-1,2,4-triazol-4-yl)diazenyl]benzene-1,3-diol

Yield: 76.24%. mp: 212-215°C. IR (KBr) cm^{-1}: 3594, 3035, 2586, 1328, 747. ^1H NMR (DMSO-d6, 400 MHz) δ: 2.49 (s, 2H, SH), 3.92 (s, 1H, OH), 6.57-7.61 (m, 1H, Ar), 7.27 (s, 1H, CH). HRMS (EI) m/z calcd for $C_{15}H_{12}N_4O_2S$ 312.35, found 312.35.

PGI 8:- 4-[(*E*)-(3-phenyl-5-sulfanyl-4*H*-1,2,4-triazol-4-yl)diazenyl]benzene-2,4-diol

Yield: 87.01%. mp: 203-205°C. IR (KBr) cm^{-1}: 3350, 3041, 2575, 1328. ^1H NMR (DMSO-d6, 400 MHz) δ: 2.49 (s, 2H, SH), 3.67 (s, 1H, OH), 6.57-7.62 (m, 1H, Ar), 7.64 (s, 1H, CH). (m, 1H, Ar). HRMS (EI) m/z calcd for $C_{15}H_{12}N_4O_2S$ 312.35, found 312.35.

PGI14:- 4-{(*E*)-[2,4-bis(trifluoromethyl)phenyl]diazenyl}-5-phenyl-4*H*-1,2,4-triazole-3-thiol

Yield: 84.32%. mp: 223-225°C. IR (KBr) cm^{-1}: 3034, 2569, 1352, 745. ^1H NMR (DMSO-d6, 400 MHz) δ: 2.47 (s, 1H, SH), 7.30-8.06 (m, 1H, Ar), 7.85 (s, 1H, CH). . HRMS (EI) m/z calcd for $C_{17}H_{10}F_6N_4S$ 416.34, found 416.34.

PGI 15:- 4-{(*E*)-[2,5-bis(trifluoromethyl)phenyl]diazenyl}-5-phenyl-4*H*-1,2,4-triazole-3-thiol

Yield: 86.20%. mp: 215-217°C. IR (KBr) cm^{-1}: 3355, 3376, 2568, 1592, 1343. ^1H NMR (DMSO-d6, 400 MHz) δ: 2.46 (s, 1H, SH), 7.39-7.62 (m, 1H, Ar), 8.14 (s, 1H, CH). HRMS (EI) m/z calcd for $C_{17}H_{10}F_6N_4S$ 416.34, found 416.34.

PGI 16:- 4-{(*E*)-[3,5-bis(trifluoromethyl)phenyl]diazenyl}-5-phenyl-4*H*-1,2,4-triazole-3-thiol

Yield: 83.52%. mp: 218-221°C. IR (KBr) cm^{-1}: 3085, 2584, 1356, 1085. ^1H NMR (DMSO-d6, 400 MHz) δ: 2.50 (s, 1H, SH), 7.35-7.62 (m, 1H, Ar), 7.77 (s, 1H, CH). HRMS (EI) m/z calcd for $C_{17}H_{10}F_6N_4S$ 416.34, found 416.34.

PGI 25:- 4-[(*E*)-(2-bromo-5-fluorophenyl)diazenyl]-5-phenyl-4*H*-1,2,4-triazole-3-thiol

Yield: 69.24%. mp: 213-215°C. IR (KBr) cm^{-1}: 3035, 2576, 1591, 744. ^1H NMR (DMSO-d6, 400 MHz) δ: 2.68 (s, 1H, SH), 7.06-7.65 (m, 1H, Ar), 7.53 (s, 1H, CH). HRMS (EI) m/z calcd for $C_{15}H_{10}BrFN_4S$ 377.23, found 377.23.

PGI 30:- 4-[(*E*)-(4-bromotetrahydrofuran-2-yl)diazenyl]-5-phenyl-4*H*-1,2,4-triazole-3-thiol

Yield: 77.21%. mp: 217-218°C. IR (KBr) cm^{-1}: 3038, 2595, 1359, 747. ^1H NMR (DMSO-d6, 400 MHz) δ: 2.37 (s, 1H, SH), 6.64-7.65 (m, 1H, Ar), 8.10 (s, 1H, CH). HRMS (EI) m/z calcd for $C_{13}H_{09}BrN_4OS$ 349.21, found 349.21.

PGI 37:- 4-bromo-2-nitro-6-[(*E*)-(3-phenyl-5-sulfanyl-4*H*-1,2,4-triazol-4-yl)diazenyl] phenol

Yield: 81.38%. mp: 221-223°C. IR (KBr) cm^{-1}: 3442, 3032, 2588, 1328. ^1H NMR (DMSO-d6, 400 MHz) δ: 2.14 (s, 1H, SH), 3.94 (s, 1H, OH), 7.29-7.68 (m, 1H, Ar),), 8.10 (s, 1H, CH). HRMS (EI) m/z calcd for $C_{15}H_{10}BrN_5O_3S$ 420.24, found 420.24.

PGI 38:- 2-[(*E*)-(3-phenyl-5-sulfanyl-4*H*-1,2,4-triazol-4-yl)diazenyl]-6-(trifluoromethyl) phenol

Yield: 82.29%. mp: 225-227°C. IR (KBr) cm^{-1}: 3456, 3040, 1341, 748. ^1H NMR (DMSO-d6, 400 MHz) δ: 2.56 (s, 1H, SH), 4.82 (s, 1H, OH), 7.13-7.75 (m, 1H, Ar) 8.10 (s, 1H, CH). HRMS (EI) m/z calcd for $C_{16}H_{11}F_3N_4OS$ 364.34, found 364.34.

PGI 43:- 5-phenyl-4-[(*E*)-(2,3,4-trimethoxyphenyl)diazenyl]-4*H*-1,2,4-triazole-3-thiol

Yield: 89.15%. mp: 209-211°C. IR (KBr) cm^{-1}: 3027, 2882, 2582, 1354. ^1H NMR (DMSO-d6, 400 MHz) δ: 2.58 (s, 1H, SH), 3.82-3.83 (s, 9H, OCH3), 7.17-7.66 (m, 1H, Ar) 8.30 (s, 1H, CH). HRMS (EI) m/z calcd for $C1_8H1_8N_4O_3S$ 370.43, found 370.43.

PGI 48:- 4-[(*E*)-(2-nitrophenyl)diazenyl]-5-phenyl-4*H*-1,2,4-triazole-3-thiol

Yield: 78.94%. mp: 214-218°C. IR (KBr) cm^{-1}: 3022, 2581, 1357, 745. ^1H NMR (DMSO-d6, 400 MHz) δ: 2.76 (s, 1H, SH), 7.36-7.87 (m, 1H, Ar), 8.49 (s, 1H, CH). HRMS (EI) m/z calcd for $C_{15}H_{11}N_5\ O_2S$ 325.32, found 325.35.

PGI 51:- 4-[(*E*)-(2-chloro-4-fluorophenyl)diazenyl]-5-phenyl-4*H*-1,2,4-triazole-3-thiol

Yield: 83.42%. mp: 223-226°C. IR (KBr) cm^{-1}: 3014, 2577, 1329, 1140, 785. ^1H NMR (DMSO-d6, 400 MHz) δ: 2.21 (s, 1H, SH), 7.07-7.68 (m, 1H, Ar), 8.31 (s, 1H, CH). HRMS (EI) m/z calcd for $C_{15}H_{10}ClFN_4S$ 332.78, found 332.78.

PGI 53:- 4-[(*E*)-(3-chloro-2-fluorophenyl)diazenyl]-5-phenyl-4*H*-1,2,4-triazole-3-thiol

Yield: 86.37%. mp: 220-222°C. IR (KBr) cm^{-1}: 3017, 2574, 1105, 749. ^1H NMR (DMSO-d6, 400 MHz) δ: 2.16 (s, 1H, SH), 7.11-7.76 (m, 1H, Ar), 7.92 (s, 1H, CH). HRMS (EI) m/z calcd for $C_{15}H_{10}ClFN_4S$ 332.78, found 332.78.

The conformation of docked molecules shows match to the space filling model of selective 1M17 co-crystalized ligand. The bulky groups in PGI series are mainly responsible for affinity binding. 15 molecules showing good binding affinity were synthesized.

CONCLUSION

4-substituted amino-5-phenyl-4H-1,2,4-triazole-3-thiol derivatives were studied by docking with an aim to reveal the structural factors responsible for 1M17 binding and selectivity. Compounds from both series exhibited good binding scores. The

molecules from each series which exhibited equivalent or better glide score were selected for synthesis and biological evaluation. Compounds showing better binding affinity were synthesized and evaluated for percentage yield, melting point, FT-IR spectroscopy, NMR spectroscopy and Mass spectroscopy. Biological evaluation will be attempted including acute toxicity studies for the synthesized compound.

CONFLICT OF INTEREST

None to declare

ACKNOWLEDGEMENTS

All authors are thankful to UGC, New Delhi for providing grants to purchase Drug Designing software (Schrodinger modeling suite) sanctioned under Major Research Project from School of Pharmacy, Swami Ramanand Teerth Marathwada University, Nanded.

REFERENCES

[1] Kallioniemi OP, Kallioniemi A, Kurisu W *et al*., ERBB2 amplification in breast cancer analyzed by fluorescence in situ hybridization, Proc Natl Acad Sci., 1992; 89: 5321–5325.

[2] Hubbard SR, Till JH, Protein Tyrosine Kinase Structure and Function, Annu Rev Biochem., 2000; 69: 373-398.

[3] Kolibaba KS, Druker BJ, Biochim. Biophys. Acta., 1997; 21: 1333.

[4] Ross JS *et al*, Targeted therapy in breast cancer: The HER-2/neu gene and protein, Mol Cell Proteomics, 2004; 3: 379 –398.

[5] Tzaha E, Waterman H, Chen X *et al*, A hierarchical network of interreceptor interactions determines signal transduction by Neu differentiation factor/ neuregulin and epidermal growth factor, Mol Cell Bio., 1996; 16: 5276–5287.

[6] Moasser MM, The oncogene HER2: Its signaling and transforming functions and its role in human cancer pathogenesis, Oncogene, 2007; 26: 6469–6487.

[7] Fleming TP, Saxena A, Ali IU, *et al*, amplification and/or over-expression of platelet-derived growth factor receptors and epidermal growth factor receptor in human glial tumors, Cancer Res., 1992; 52: 4550.

[8] Anido J, Matar P, Albanell J *et al*, ZD1839, A specific epidermal growth factor receptor (EGFR) tyrosine kinase inhibitor, induces the formation of inactive EGFR/HER2 and EGFR/HER3 heterodimers and prevents heregulin signaling in HER2-overexpressing breast cancer cells, Clin. Cancer Res., 2003; 9: 1274.

[9] Mona M. Kamel, Nadia Y. Megally Abdo, Synthesis of Novel 1,2,4-triazoles, Triazolothiadiazines and Triazolothiadiazoles as Potential Anticancer Agents, European Journal of Medicinal Chemistry, 2014; 86: 75-80.

[10] www.rcsb.org.

[11] Zerong Wang, Comprehensive Organic Name Reactions and Reagents, 1095-1097.

[12] Amol D. Sonawane, Navnath D. Rode, LaxmanNawale, Rohini R. Joshi, Ramesh A. Joshi, Anjali P. Likhite, Dhiman Sarkar.Synthesis and biological evaluation of 1, 2, 4- triazole 3-thione and 1, 3, 4 Oxadiazole thione as anti-mycobacterial agents. (2016).